C. R. Mecanique 341 (2013) 266–276

Contents lists available at SciVerse ScienceDirect

Comptes Rendus Mecanique

www.sciencedirect.com

Combustion, flow and spray dynamics for aerospace propulsion

Data assimilation applied to combustion

Assimilation de données en combustion

Mélanie C. Rochoux [a,c,d,*], Bénédicte Cuenot [a], Sophie Ricci [b], Arnaud Trouvé [e], Blaise Delmotte [b,e], Sébastien Massart [b], Roberto Paoli [b], Ronan Paugam [f]

[a] *CERFACS, 42, avenue Gaspard-Coriolis, 31057 Toulouse cedex 01, France*
[b] *URA CERFACS-CNRS, URA-1875, 42, avenue Gaspard-Coriolis, 31057 Toulouse cedex 01, France*
[c] *École centrale Paris, grande voie des vignes, 92295 Châtenay-Malabry, France*
[d] *UPR EM2C-CNRS, UPR-288, grande voie des vignes, 92295 Châtenay-Malabry, France*
[e] *Department of Fire Protection Engineering, University of Maryland, College Park, MD 20742, USA*
[f] *Department of Geography, King's College London, Strand, London, WC2R 2LS, UK*

ARTICLE INFO

Article history:
Available online 9 January 2013

Keywords:
Combustion
Data assimilation
Fire propagation

Mots-clés :
Combustion
Assimilation de données
Propagation de feux

ABSTRACT

Data assimilation is a sophisticated technique, yet not available in combustion, that combines measurements to model simulation and account for uncertainties in order to improve the numerical prediction of a system. In the context of gas turbines, data assimilation may be used for example to improve the prediction of flame ignition and propagation by a smart analysis of images and measurements. A first illustration of data assimilation is given in a simple case, where synthetic time-evolving positions of the flame front are assimilated to calibrate parameters of a premixed flame model. Its successful application in the context of natural fire propagation assesses the predictive capacity of the technique and the resulting higher fidelity in the data-driven simulations.

RÉSUMÉ

L'assimilation de données, encore inappliquée en combustion, combine mesures et simulations en tenant compte des incertitudes afin d'améliorer la prévision numérique d'un système. Dans le contexte des turbines à gaz, l'assimilation de données peut être utilisée par exemple pour améliorer l'estimation de l'allumage et de la propagation de la flamme, grâce à une exploitation plus poussée de données telles que des images ou des mesures ponctuelles. Une première illustration de l'assimilation de données est présentée pour la prédiction de la propagation d'un front de flamme dans un cas test simple. Dans cet exemple, les positions du front de flamme au cours du temps sont assimilées pour caler les paramètres d'un modèle de flamme prémélangée. La capacité de prédiction des simulations obtenues par assimilation de données est finalement démontrée dans un cas réel de propagation de feux naturels.

* Corresponding author at: CERFACS, 42, avenue Gaspard-Coriolis, 31057 Toulouse cedex 01, France.
E-mail addresses: melanie.rochoux@ecp.fr (M.C. Rochoux), cuenot@cerfacs.fr (B. Cuenot), ricci@cerfacs.fr (S. Ricci), atrouve@umd.edu (A. Trouvé).

1631-0721/$ – see front matter
http://dx.doi.org/10.1016/j.crme.2012.10.011

1. Introduction

Computational Fluid Dynamics (CFD) models cannot perfectly describe a physical system and its evolution, because of uncertainties on the physical and numerical parameters as well as uncertainties related to the simplification and discretization of the physics and to the numerical methods. On top of these errors, initial and boundary conditions are also a source of significant uncertainties that can accumulate over time. Such limitations may be partly overcome by coupling information coming from both measurements and simulations, taking into account that none of them, when used alone, provides a certain and complete description of the real state of the system. The idea is to use observations to best estimate the set of parameters, or initial/boundary conditions for the model to improve its accuracy and reliability. Data assimilation (DA) offers the adequate framework to perform such combination of data and simulation and thus, to solve this inverse problem [1]. This technique consists in incorporating data into a running model in such way as to minimize the error, using estimated statistical errors on both simulated and observed data [2,3]. It fits into the wider domain of dynamic data-driven application systems, where data are used to formulate some feed-back information on the system, leading to the reduction of uncertainties on the model and its outputs.

The benefit of data assimilation has already been greatly demonstrated in meteorology [4] and oceanography [5] over the past decades, especially for providing initial conditions for numerical forecast. It is now being used increasingly in various fields of application such as hydrology, atmospheric chemistry or oil reservoir modeling. Introducing this approach in combustion would mean to use measurements (images or probe signals) to reduce uncertainties on, for example, the turbulent flame speed or the heat transfer to the walls. This could also be applied to unsteady processes such as burner ignition or extinction. It may directly improve simulation results, through improved initial and/or boundary conditions (spray injection, wall temperatures, etc.), or improve physical models when applied to parameters. DA can also be used to dynamically optimize an observation network [6]. In combustion, this could be used, for example, to optimize the place and time of probe measurements, in order to obtain the best characterization of a system given a set of equipments.

The objective of the present work is to illustrate how DA techniques can be applied to CFD, and to demonstrate their merits and potential benefits. More precisely, DA is used here to achieve a data-driven model parameter estimation for flame propagation. In the simplified model of premixed flame, a progress variable is used to identify an interface between burned and fresh fuel, propagating at the local flame speed. In this formulation, the local flame speed is linked to the local mixture and flow conditions. The DA algorithm aims at correcting the input parameters, which are significant sources of uncertainties in the estimation of the flame speed. Observations of the front positions are assimilated using a simplified Kalman Filter algorithm [3]: the DA approach is applied over a time window, during which several observations of the front location are available and the model parameters are assumed to remain constant.

As a first step, DA is applied to a simplified and synthetical case of premixed flame propagation. In this case, the correction focuses on a single input parameter, which encompasses different physical processes and assumptions, sources of significant uncertainties but not distinguished here. The DA methodology is then illustrated on a real case of wildfire propagation, for which several input parameters, characterizing the vegetation, are poorly known. The application of DA in the context of wildfire modeling has been considered only recently; Mandel et al. [7] used an Ensemble Kalman Filter technique to calibrate successfully the temperature field state of a wildfire model, by assimilating temperature measurements, even though the ignition location was poorly described. Our objective here is to integrate airborne observations of fire front positions into a fire spread model in order to obtain an optimal set of model parameters. The simplified Kalman Filter algorithm is indeed able to provide a correction specific to each control parameter, leading to a better tracking of the heterogeneities of the considered physical system.

The outline of the article is as follows: Section 2 describes the mathematical material for data assimilation as well as the algorithm used, in this study, to correct the flame speed. Section 3 provides the description and the validation of the model of flame propagation. In Section 4, the DA approach is first validated on an Observation System Simulation Experiment (OSSE) case: the true state of the system is assumed to be known, and the observations are synthetically-generated using this true state. Then, the DA algorithm is applied to a real case of fire propagation, using thermal-infrared images of the fire, to correct parameters, characterizing the vegetation properties in the formulation of the rate of spread.

2. Principles of data assimilation for parameter calibration

2.1. The variables of interest

The calibration of the model parameters can be formulated as an inverse problem, conveniently solved in the framework of data assimilation. It combines model simulation and observational information in order to approximate as best as possible the real parameters of the model, and hence improve the description of the system. The outline of the DA algorithm, as well as the required mathematical quantities are represented in Fig. 1 and are now listed:

(i) **A control vector $\mathbf{x}$** – The DA algorithm identifies the optimal estimate of the true value $\mathbf{x}^t$ of an unknown variable $\mathbf{x}$. In the context of this study, the control vector $\mathbf{x}$ includes n model parameters. Starting from an a priori value of the control parameters, called the background vector and denoted by $\mathbf{x}^b$, and given a set of observations denoted

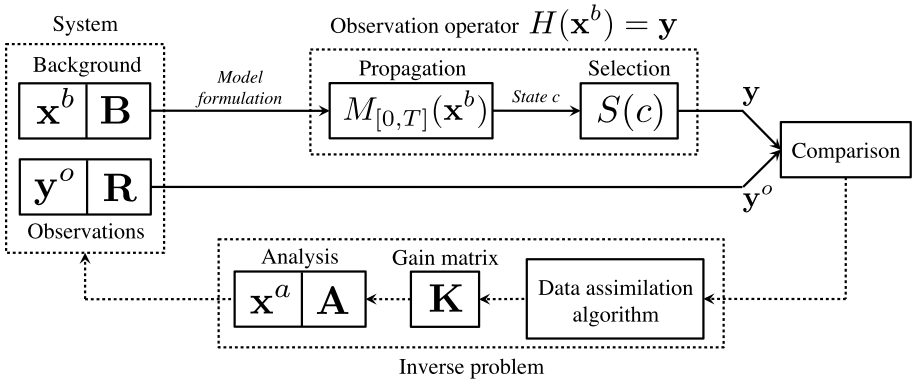

Fig. 1. Schematic representation of the DA algorithm on the $[0, T]$ time window.

by $\mathbf{y}^o$, DA is aimed at identifying the optimal estimation of $\mathbf{x}^t$, called the analysis vector $\mathbf{x}^a$. This estimate is a feedback information for the model. It is optimal when the variance of its distance to $\mathbf{x}^t$ gets a minimum, meaning, for Gaussian cases, that its probability density function is dense around its mean.

(ii) **An observation vector $\mathbf{y}^o$** – It is a set of p measurements made over the assimilation time window $[0, T]$. In this study, the observed quantity is the time-evolving location of the flame front, obtained at the different observation times of this time window. $\mathbf{y}^o$ gathers therefore the 2-D coordinates of the $p/2$ points located on the observed fronts (one measurement for each of the two coordinates of the points, leading to an observation vector of p elements).

(iii) **An observation operator** $H(\mathbf{x})$ – It maps the control space onto the observation space. The construction of the observation operator $H(\mathbf{x})$ is a two-step operation as $H(\mathbf{x})$ is the composition of a numerical model $M_{[0,T]}(\mathbf{x})$, and of a selection operator $S(c)$:

- **The numerical model** $M_{[0,T]}(\mathbf{x})$ integrates the physics on the assimilation time window $[0, T]$, using the control vector $\mathbf{x}$ of model parameters. It provides therefore the simulated field associated to $\mathbf{x}$, denoted by the variable c in this study.
- **The selection operator** $S(c)$ – A flame front is represented, here, by an isocontour of the field variable c. So the selection operator extracts, from the simulated field c, the isocontours at the observation times of the time window $[0, T]$.

(iv) **The tangent linear H of the observation operator** – The DA algorithm requires the formulation of the gain matrix $\mathbf{K}$ in order to account for the sensitivity of the flame front position to change in the control parameters $\mathbf{x}$ and thus to quantify the required correction to $\mathbf{x}$. The gain matrix $\mathbf{K}$ involves therefore the Jacobian of the observation operator H. Since this operator is usually not available analytically, it is identified as the Jacobian matrix in the Taylor expansion of the observation operator, in the vicinity of a reference control vector $\mathbf{x}_{ref}$, usually chosen as the background; this Jacobian matrix, called the tangent linear and denoted by $\mathbf{H}$, is only valid locally, in the vicinity of $\mathbf{x}_{ref}$. In practice, $\mathbf{H}$ is calculated by simple differentiation after perturbing each element of the control vector $\mathbf{x}_{ref}$ and evaluating the corresponding change in the observation operator $H(\mathbf{x}_{ref})$.

(v) **The background and observation error covariance matrices B and R** – In most data assimilation algorithms, the background error $\boldsymbol{\epsilon}^b$ and observation error $\boldsymbol{\epsilon}^o$ statistics are described by Gaussian probability density functions $\mathcal{N}$ with a zero mean value and an error covariance model.

- The background $\mathbf{x}^b$ provides, prior to data assimilation, a first estimation of $\mathbf{x}^t$ with an uncertainty $\boldsymbol{\epsilon}^b$, such that $\mathbf{x}^b = \mathbf{x}^t + \boldsymbol{\epsilon}^b$, with $\boldsymbol{\epsilon}^b \sim \mathcal{N}(0, \mathbf{B})$. The background error covariance matrix $\mathbf{B}$ is a square symmetric matrix of size $n \times n$, where the diagonal elements represent the error variance $(\sigma^b)^2$ for each control parameter, while the off-diagonal terms stand for the covariances between the parameters errors. These off-diagonal terms are assumed to be negligible in the following, so that $\mathbf{B}$ is reduced to a diagonal matrix.
- Similarly for the observations $\mathbf{y}^o$, satisfying $\mathbf{y}^o = H(\mathbf{x}^t) + \boldsymbol{\epsilon}^o$, the observation error $\boldsymbol{\epsilon}^o$ follows a Gaussian distribution $\mathcal{N}(0, \mathbf{R})$. The observation error covariance matrix $\mathbf{R}$ is a square symmetric matrix of size $p \times p$. Classically, observational measurements are assumed to have uncorrelated errors in space and time. $\mathbf{R}$ is therefore reduced to a diagonal matrix of p elements, each element representing the error variance $(\sigma^o)^2$ of the position of the observed fronts.

2.2. The Best Linear Unbiased Estimator (BLUE) algorithm

The BLUE algorithm is derived from the Kalman Filter approach [8–10]. It formulates the optimal analysis $\mathbf{x}^a$ as a correction of the background $\mathbf{x}^b$ [3], under the assumption that the observation operator is linear. It also provides the analysis error covariance matrix $\mathbf{A}$, whose diagonal elements are the error variance $(\sigma^a)^2$ of each control parameter. The analysis reads

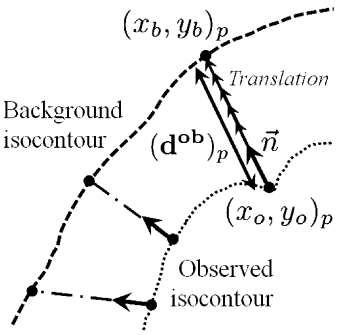

Fig. 2. Formulation of the innovation vector $\mathbf{d}^{ob}$.

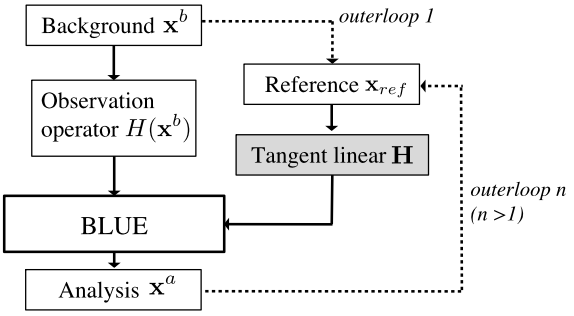

Fig. 3. DA algorithm as a BLUE iterative process.

$$\mathbf{x}^a = \mathbf{x}^b + \mathbf{K}\underbrace{\left(\mathbf{y}^o - H\left(\mathbf{x}^b\right)\right)}_{\mathbf{d}^{ob}} \tag{1a}$$

$$\mathbf{A} = (\mathbf{I} - \mathbf{KH})\mathbf{B} \tag{1b}$$

In Eq. (1a), the corrective term $\mathbf{Kd}^{ob}$ directly depends on the distance, called the innovation vector $\mathbf{d}^{ob}$, between the observations $\mathbf{y}^o$ and the image of the background in the observation space $H(\mathbf{x}^b)$. This difference is weighted by the gain matrix $\mathbf{K} = \mathbf{BH}^T(\mathbf{HBH}^T + \mathbf{R})^{-1}$, which depends on both background and observation error statistics (via $\mathbf{B}$ and $\mathbf{R}$) as well as on the tangent linear $\mathbf{H}$.

In this study, the formulation of the innovation vector $\mathbf{d}^{ob}$ consists in computing the time-evolving distance between two fronts, the observed front and the simulated front associated to the background parameters $\mathbf{x}^b$. In practice, at each observation time, this distance is computed by projecting, along the normal direction, each point of the observed front onto the simulated isocontour (see Fig. 2). Such a definition of the distance allows to capture the topology of the front and thereby the inhomogeneities in the front propagation.

The BLUE algorithm can be extended to non-linear observation operators: the BLUE solution is iterated using the analysis as the new reference vector $\mathbf{x}_{ref}$ for the formulation of the tangent linear $\mathbf{H}$. This iterative process, named external loop (or outerloop), is presented in Fig. 3. It enables to take into account some non-linearities in the observation operator, leading to a good estimation of the optimal control vector for the non-linear problem, using a simple DA algorithm. This approach can lead to three potential scenarii, schematized in Fig. 4: (a) a perfect confidence in the background $\mathbf{x}^b$ leads to $\mathbf{x}^a = \mathbf{x}^b$; (b) on the opposite, for a perfect confidence in the observations $\mathbf{y}^o$, the time-evolving flame fronts associated to the analysis $\mathbf{x}^a$ match well with the observed fronts; and (c) if both background and observations have a significant uncertainty, then the analysis $\mathbf{x}^a$ provides an intermediate solution between the background and the observations. These scenarii highlight how DA combines information from both model and measurements (in terms of data and uncertainties) to obtain more realistic control parameters than if either of them were taken separately.

2.3. The Observation System Simulation Experiment (OSSE)

The optimality of the analysis can be ensured using the OSSE framework, schematized in Fig. 5. It provides a powerful tool to quantify the quality of the correction to the background, and thus to validate the proposed DA prototype.

In this context, the true control vector $\mathbf{x}^t$ is supposed to be known. The observations over the assimilation time window $[0, T]$ are synthetically-generated using the numerical model $M_{[0,T]}(\mathbf{x}^t)$ and the true value of the control parameters $\mathbf{x}^t$. Operating on the resulting trajectory $c(\mathbf{x}^t)$, the selection operator leads to the extraction, at each observation time, of the points located along the simulated isocontours $c = 0.5$. A random noise $\boldsymbol{\epsilon}^o$ of zero mean and of standard deviation σ^o is

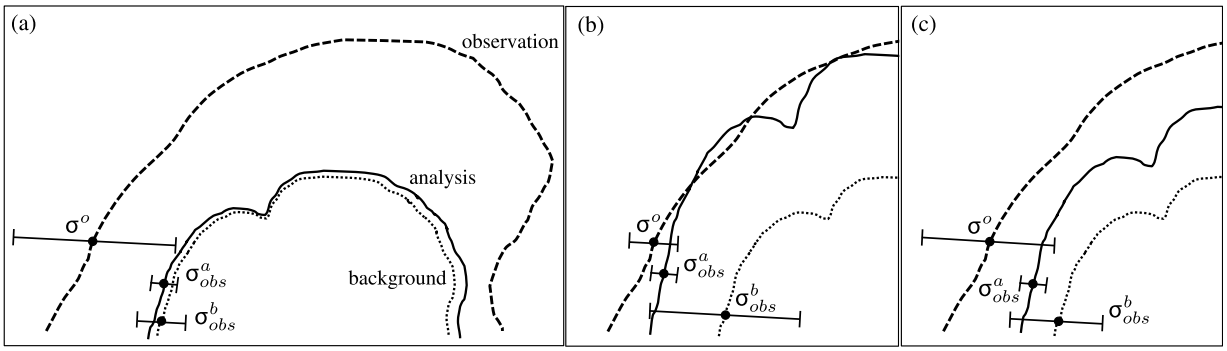

Fig. 4. Schematic comparison, at a given observation time, of the flame fronts (associated to the observation in dashed line, background in dotted line and analysis in plain line), along with their respective standard deviation error σ^o, σ^b_{obs} and σ^a_{obs} (σ^b_{obs} and σ^a_{obs} representing the standard deviation error in the control parameters projected onto the observation space), for the 3 potential scenarios in DA: (a) a high confidence in the background; (b) a high confidence in the observations; (c) a significant uncertainty in both background and observations.

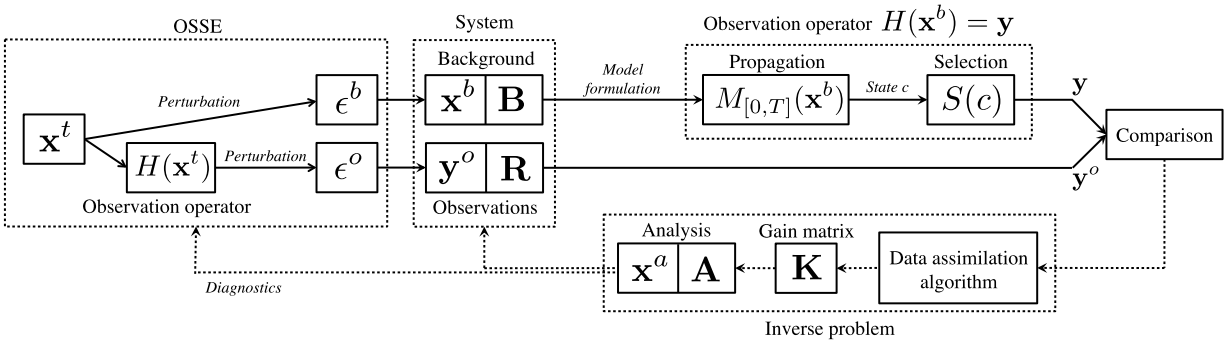

Fig. 5. OSSE framework for the data assimilation algorithm on the $[0, T]$ time window.

then added at each front point position to account for observation error and thus, to define the observation vector $\mathbf{y}^o$. To define the background vector $\mathbf{x}^b$, a perturbation $\boldsymbol{\epsilon}^b$ of zero mean and of standard deviation σ^b is added to the true value of the control vector $\mathbf{x}^t$. In this OSSE framework, the true control vector $\mathbf{x}^t$ as well as the observation and background errors $\boldsymbol{\epsilon}^o$ and $\boldsymbol{\epsilon}^b$ are known; diagnostics comparing $\mathbf{x}^a$ and $\mathbf{x}^t$ can therefore be developed and used as validation tools of the proposed DA prototype.

3. Model for flame propagation

The observation operator $H(\mathbf{x})$ stands in the time-integration of a flame propagation model $M_{[0,T]}(\mathbf{x})$, which, for a given set of control parameters $\mathbf{x}$, provides the time-evolving locations of the flame front once applied the selection operator. Such a simulation requires (1) a model for the premixed flame speed s_L for heterogeneous fuel conditions; and (2) a simulator of front propagation, which propagates the flame at the proposed s_L.

3.1. Level-Set method as front-tracking technique

A premixed flame propagates at a velocity s_L toward the unburned fuel, which is, prior to ignition, a mixing of both oxidizer and fuel. It is classically represented by a scalar progress variable c, varying from $c = 1$ in the burned gases to $c = 0$ in the fresh gases [11]. Located at their interface, the flame front is defined here as the isocontour $c = 0.5$ (see Fig. 6). The shape of this isocontour is related to the fuel distribution, described by a mass fraction variable Y_F, which is a dimensionless variable varying randomly between 0 and 1 along the 2-D computational domain.

The isocontour $c = 0.5$ is propagated using a Level-Set method, based on a second-order Runge–Kutta scheme for time-integration and a second-order MUSCL (Monotone Upstream-centered Schemes for Conservation Laws) technique with a Superbee slope limiter for spatial discretization. Details of the numerical method are given in Rehm and McDermott [12]. In this context, the progress variable c satisfies

$$\frac{\partial c}{\partial t} + \mathbf{u} \cdot \nabla c + \mathbf{s}_L \cdot \nabla c = 0 \tag{2}$$

where $\mathbf{u}$ is the flow velocity and $s_L = \mathbf{s}_L \cdot \mathbf{n}$ is the flame speed (in the reference frame of the flame) along the normal direction $\mathbf{n}$.

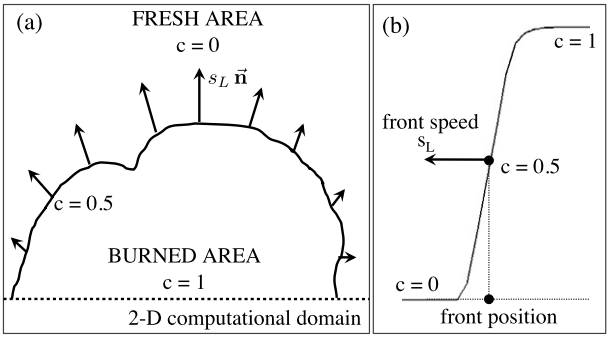

Fig. 6. Premixed flame model: (a) propagation of the front along a 2-D surface; (b) profile of the progress variable c.

The physics of the flame spread is assumed to be exclusively included in the formulation of s_L; s_L being parameterized in terms of a reduced number of parameters that characterize the fuel properties. s_L is defined here as a linear function of the fuel mass fraction Y_F. In a preliminary step, the proportionality parameter P [m/s] does not distinguish the different physical processes taken into account in the modeling of s_L. It satisfies the following equation:

$$s_L(x, y) = P \times Y_F(x, y) \tag{3}$$

3.2. Numerical configuration

For the DA illustration in the OSSE context (presented in Section 4.1), only the proportionality coefficient P is calibrated, so that $\mathbf{x} = P$. The true simulation is defined assuming that the true value of this control parameter is $P^t = 0.1$ m/s. It propagates a semi-circular front over a 2-D domain of 300 m $\times$ 300 m (with a step size $\Delta x = \Delta y = 1$ m), which represents a horizontal fuel layer characterized by a random mass fraction Y_F, as illustrated in Fig. 7(a). There is no external flow ($\mathbf{u} = 0$). The initial condition is described by a semi-circular front centered in ($x_0 = 150$ m, $y_0 = 0$ m) and of radius $r_0 = 5$ m. Eq. (2) is integrated during 800 s, Fig. 7(b) displays the isocontour $c = 0.5$, each 200 s, starting from the initial condition.

Diagnostics on the flame speed and thickness, derived from the Kolmogorov–Petrovsky–Piskounov (KPP) analysis [11] and extrapolated to heterogeneous fuel, have been developed to validate the flame propagation model. In Fig. 7(c), the rate of change of the progress variable c over the 2-D computational domain, denoted by s_L^d, matches the average speed of the front s_L^*. This means that the front propagates at the prescribed s_L, defined by Eq. (3). Also, it was verified that the flame thickness δ_L^d, estimated as the average inverse of the maximum gradient of c, remains small and relatively constant over time (see Fig. 7(c)).

4. Data assimilation experiments for flame propagation

4.1. Validation case – Correction of the flame speed

The DA prototype is applied in the context of OSSE for validation. The control parameter $\mathbf{x}$ is composed of the model parameter P, with the true value defined as $\mathbf{x}^t = P^t = 0.1$ m/s. For this single parameter calibration, the background error covariance matrix $\mathbf{B}$ sums up to the variance $(\sigma^b)^2$ of the error on the background value P^b. The analysis is performed for different values of P^b ranging from 0.02 to 0.18 m/s. The associated error $\boldsymbol{\epsilon}^b = P^t - P^b$, used to prescribe the error standard deviation of the background σ^b, varies therefore from -80% to $+80\%$ of $\mathbf{x}^t$. The observed fronts are discretized with 200 points, and there are 16 observation times each 50 s along the assimilation time window [0, 800 s]. The observation error standard deviation is set to $\sigma^o = 0.0073$ m to prescribe a high level of confidence in the observations. The observations are therefore representative of the true isocontours.

Diagnostics on the analysis are established in the control space and in the observation space. In the control space, for all tested values of the background parameter $\mathbf{x}^b$, the assimilation process retrieves the true value $\mathbf{x}^t$ of the parameter P, within less than 0.1%, for a very low number of external loops (2 or 3). More importantly, this process systematically reduces the error variance on P by several orders of magnitude. For instance, when the background error is $+80\%$ of $\mathbf{x}^t$, $(\sigma^b)^2 = 6.4 \times 10^{-3}$ and $(\sigma^a)^2 = 10^{-13}$. This means that the BLUE algorithm provides, as expected from Eq. (1b), a control parameter with an uncertainty that is significantly reduced compared to the background. In the observation space, the standard deviation (STD) of the distance between simulated fronts and observed fronts, calculated over the whole assimilation time window [0, 800 s], is significantly reduced using data assimilation. This is illustrated in Fig. 8, where OMB (Observation Minus Background) represents the distance between the observed fronts and the simulated fronts using $\mathbf{x} = \mathbf{x}^b$ (without data assimilation), while OMA (Observation Minus Analysis) represents the distance between the observed fronts and the simulated fronts using $\mathbf{x} = \mathbf{x}^a$ (with data assimilation). In all cases, STD(OMA) takes values that are orders of magnitude

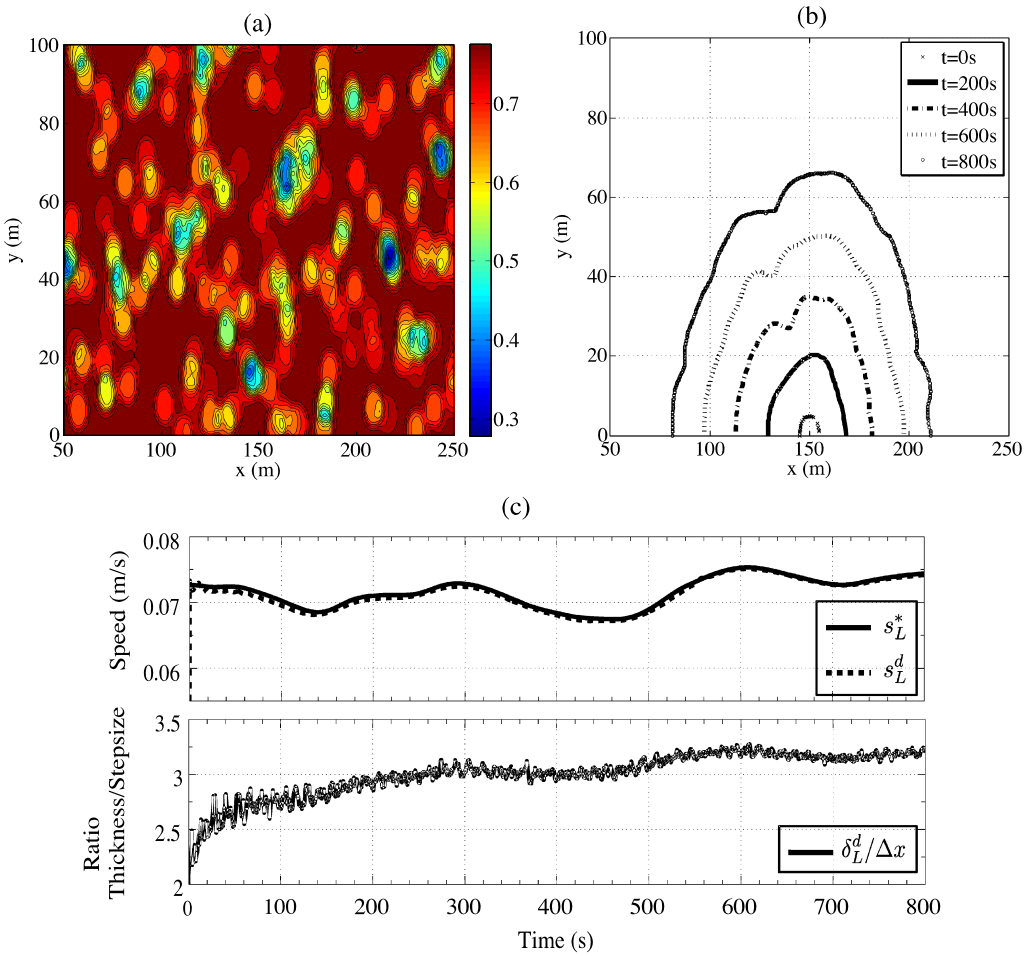

Fig. 7. (a) Random distribution of the fuel mass fraction Y_F; (b) time-evolving isocontours $c = 0.5$ for the numerical simulation associated to $P = 0.1$ m/s; (c) simulation diagnostics. Top: Average flame speed diagnostic s_L^d (m/s) in dotted line and model s_L^* (m/s) in plain line. Bottom: Ratio of the flame thickness δ_L^d (m) to the mesh step size $\Delta x = 1$ m.

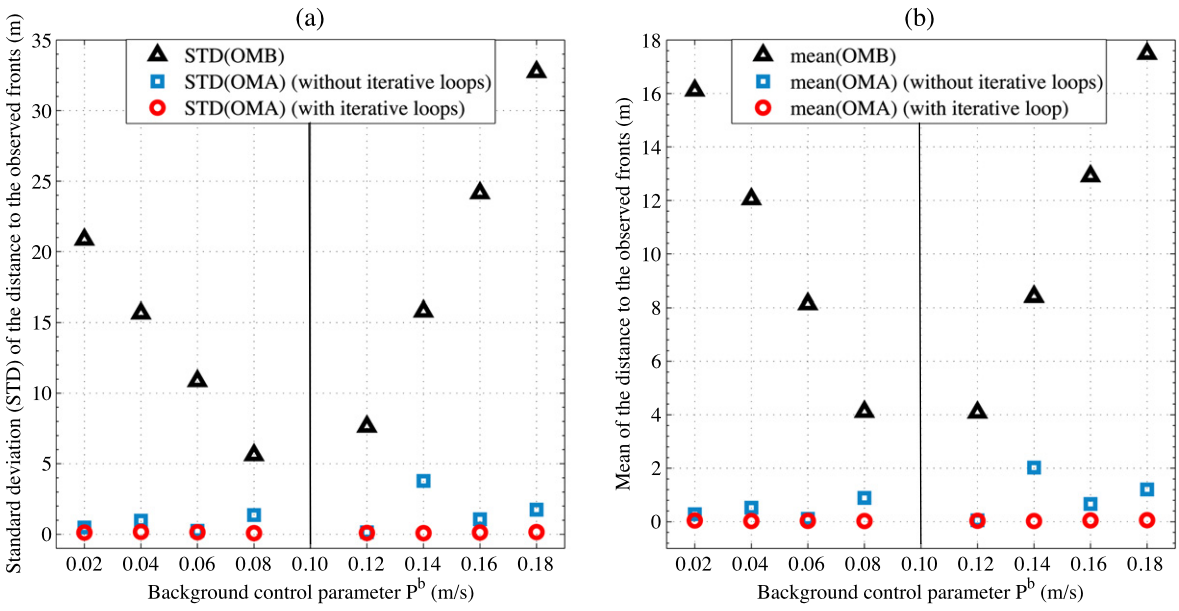

Fig. 8. OMB/OMA comparison in terms of (a) standard deviation (STD); and (b) mean.

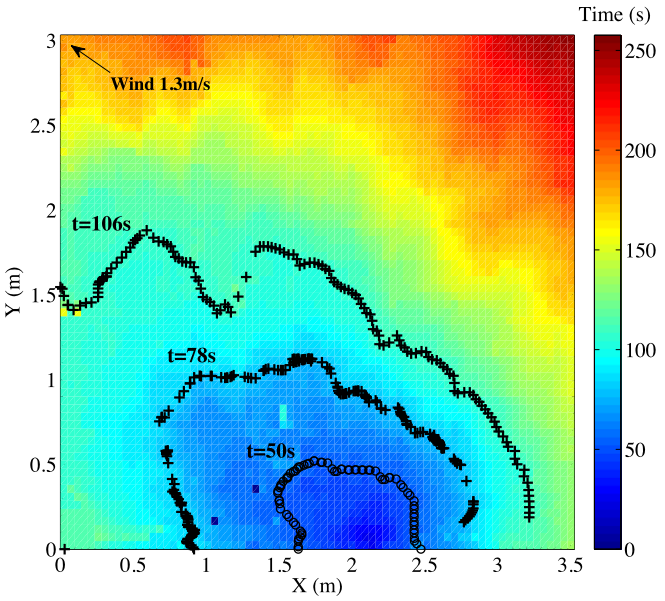

Fig. 9. Arrival times of the fire front.

smaller than STD(OMB). This is also verified for the mean of the distance between simulated fronts and observed fronts, with mean(OMA) < mean(OMB).

This series of assimilations in the context of OSSE assesses the quality of the DA algorithm since it is able to retrieve the true flame speed for a large range of perturbations, even though the observation operator is non-linear. It shows that the assimilation of front-like observations can successfully be used to obtain a better estimate of the flame speed at the end of the assimilation time window.

4.2. Real case application

This DA prototype is illustrated in the context of natural fire propagation, out of the OSSE context, for the calibration of several physical parameters involved in the formulation of the flame speed. Real data from an experimental grassland fire are assimilated in order to forecast more accurately how the flame will evolve further in time.

4.2.1. Real observations of a controlled grassland fire spread

In this experiment, the fire propagates over a domain of 4 m × 4 m under moderate wind conditions that are assumed to be uniform and constant, $v = 1.3$ m/s blowing into a western direction ($\alpha = 307$ degree in the reference frame of the picture). The grass has homogeneous properties, a uniform thickness $\delta = 8$ cm and moisture content $M_f = 22\%$. The fire spread was recorded during 350 s using a thermal-infrared camera; the resulting observations are the time-evolving positions of the fire front (see Fig. 9), which are identified as the zones where the temperature gradient is maximal. Details of the measurement technique are given in Wooster et al. [13]. The measured mean rate of spread is between 0.015 and 0.020 m/s; the maximum value being reached when the fire front spreads in the same direction as the wind, i.e. between the fire ignition ($t = 0$ s) and time $t = 120$ s.

4.2.2. Model for the fire rate of spread

At a macroscopic scale, the propagation of a grassland fire over a 2-D vegetal bed can be described using the model of premixed flame presented in Section 3, by substituting the flame speed $\mathbf{s}_L$ in the flame frame of reference by the apparent flame rate of spread $\boldsymbol{\gamma}$ (e.g., $\boldsymbol{\gamma} = \mathbf{u} + \mathbf{s}_L$). In this context, the progress variable c satisfies:

$$\frac{\partial c}{\partial t} + \boldsymbol{\gamma} \cdot \nabla c = 0 \tag{4}$$

Following Rothermel's approach [14], the idea is to include all the modeled physical processes in the parameterization of the rate of spread Γ ($\Gamma = \boldsymbol{\gamma} \cdot \mathbf{n}$, with $\mathbf{n}$ the normal direction to the fire front). Γ is therefore a parametric function of the vegetation characteristics (typically, the vegetation moisture content M_f, the surface-area-to-volume ratio of the fuel particles Σ and the vegetation layer depth δ), and of the wind velocity projected along the local normal direction to the front, denoted by $\mathbf{u}$ and satisfying $\mathbf{u} = \mathbf{v} \cdot \mathbf{n}$, with $\mathbf{v} = (v \sin\alpha, v \cos\alpha)^T$. The rate of spread Γ reads:

$$\Gamma(x, y, t) = P\big(\mathbf{u}(x, y, t), M_f, \Sigma\big)\delta \tag{5}$$

Table 1
Data assimilation results for the natural fire application, with the control vector $\mathbf{x} = (M_f, \Sigma)^T$.

Trajectory	Control vector	Parameter error standard deviation	Observed time	Distance to the observed front
Background	$\mathbf{x}^b$	σ^b	t_{obs}	mean(OMB)/STD(OMB)
	22%	6.63%	78 s	0.376 m/0.099 m
	4921 m^{-1}	1449 m^{-1}	106 s	0.784 m/0.181 m
Analysis	$\mathbf{x}^a$	σ^a	t_{obs}	mean(OMA)/STD(OMA)
	11%	0.34%	78 s	0.099 m/0.084 m
	13 193 m^{-1}	400 m^{-1}	106 s	0.147 m/0.130 m

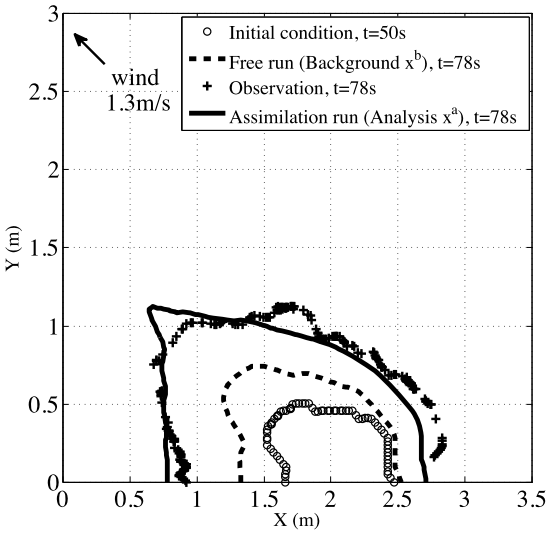

Fig. 10. Assimilation at $t = 78$ s.

For the characteristics of the real fire (e.g., $\delta = 8$ cm, $v = 1.3$ m/s, $M_f = 22\%$, $\Sigma = 4921$ m^{-1}), this model gives in the wind direction the rate of spread $\Gamma = 0.010$ m/s. This rate of spread underestimates the observed measurements and needs to be corrected to better track the fire front over time.

4.2.3. Data assimilation results

The objective is to calibrate the two vegetal parameters $\mathbf{x} = (M_f, \Sigma)^T$ in order to obtain an optimal rate of spread Γ for the experimental conditions. Out of the OSSE context, the true value of the control parameters is not known; a first guess for the parameters (e.g., the background) can be formulated using the field measures ($M_f^b = 22\%$) and Rothermel's model ($\Sigma^b = 4921$ m^{-1} for grass-like vegetation [14]). The background error is also difficult to estimate, an uncertainty of 30% is arbitrarily prescribed in both parameters to define their error standard deviation σ^b.

As to the observations, a specific data treatment was required to adapt them to the computational domain. The initial condition for the simulation is taken to be the observed state of the fire at $t = 50$ s (see Fig. 9). Only one isocontour, corresponding to $t = 78$ s, is assimilated, and the error standard deviation of the front location is prescribed in accordance to the spatial resolution of the thermal-infrared camera, namely $\sigma^o = 0.047$ m.

Using this data assimilation configuration on the time window [50, 78 s], the BLUE algorithm (with 3 external loops) leads to the analysis $\mathbf{x}^a = (11\%, 13193\ m^{-1})^T$, as shown in Table 1. It shows primarily that the error standard deviation of the analysis σ^a is reduced by one order of magnitude compared to the background error standard deviation σ^b for each parameter. Out of the OSSE context, the only diagnostic which can be established on the value of the control parameters is linked to their physical meaning: M_f^a and Σ^a are still within their physical range, but Σ^a is far from the typical value [14]. If the control space is enlarged to more parameters, the BLUE algorithm will provide a more physical value for each parameter, the tangent linear being able to correct each parameter specifically. Indeed, the present correction in M_f and Σ is overestimated to compensate for the uncertainties in the other parameters of the rate of spread. Hence, the DA algorithm should be applied to an extended control vector to provide more realistic values of the control parameters. Still, this work already outlines that the analysis leads to the improvement of the simulations of the fire spread.

Effectively, given the high level of confidence in the observed front, the optimization process finds the parameters that enable the analysis front to be a good approximation of the observed front at $t = 78$ s. Fig. 10 shows indeed that, at this time, the analysed front is much closer to the observation than the background front. More quantitatively, both diagnostics STD(OMA) < STD(OMB) and mean(OMA) < mean(OMB) are satisfied in Table 1 as expected from the OSSE study. However,

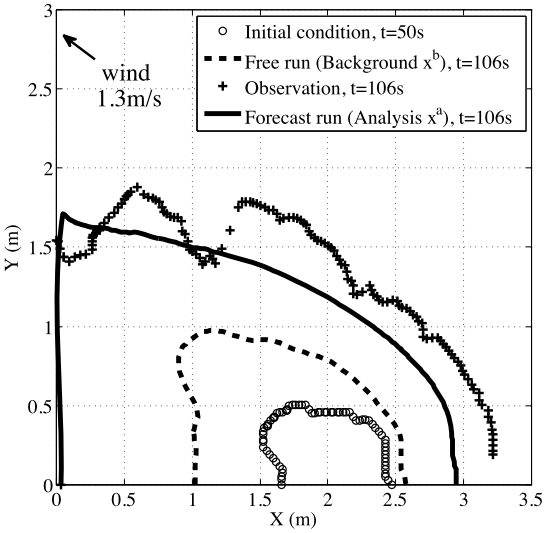

Fig. 11. Forecast at $t = 106$ s.

in such a multi-dimensional parameter space, several set of parameters may provide the same simulated front close to the observed front at the end of the assimilation time window. Even though there may exist other solutions, the BLUE algorithm guarantees the optimality of the analysis for the linear problem, and gives therefore a good candidate for the non-linear problem, in the sense that it provides parameters that, to some extend, remain close to the background and simulations that are in much better accordance with the observations. The equifinality problem would be reduced by extending the control space, that is to say by increasing the number of constraints in the optimization process and thus, by reducing the number of potential set of parameters for the analysis $\mathbf{x}^a$.

The set of estimated parameters $\mathbf{x}^a$ can be used to simulate the front propagation further in time. Here, a forecast of the fire spread is performed at $t = 106$ s, one assimilation time window after the analysis is obtained. Fig. 11 shows that the analysis front provides a better tracking of the observed front than the background front, this is consistent with the conditions STD(OMA) < STD(OMB) and mean(OMA) < mean(OMB) in Table 1. However, the data-driven simulation deviates from the observed front during the forecast, the analysis could therefore be used as the background of the next assimilation time window, and successive assimilations could be implemented in order to refine progressively the value of the control parameters in accordance to the fire spread conditions. Strong heterogeneities in the fuel or variations in the wind direction could highly strengthen the time-dependent behavior of the fire. So the size of the assimilation time window should be adapted to make sure that the control parameters could be assumed constant over this time window.

5. Conclusions

The present investigation highlights how the data assimilation (DA) approach is able to improve the prediction of fire spread using measurements of the fire front time-evolving positions. Based on a Kalman Filter algorithm, the proposed DA procedure was able to retrieve more accurate values of parameters in the flame speed model, resulting in more accurate forecasts of the fire front propagation.

Such a technique could be applied to gas turbine simulations, where numerical models have substantive sources of uncertainties such as initial/boundary conditions and other input parameters. For example, flame front observations in a burner, obtained with thermal-infrared visualizations or Laser-Induced Fluorescence (LIF) of the OH radical, could be used for a DA approach with LES simulation of the burner, to improve the accuracy of the results or the turbulent combustion model. By integrating measurements, along with their uncertainties, into simulations, DA provides a new and powerful framework to relate experiments and numerical solutions in a comprehensive way, as it is highly needed but not yet available in the combustion field.

References

[1] A. Tarantola, Inverse Problem Theory, Methods for Data Fitting and Parameter Estimation, Elsevier, 1987.
[2] K. Ide, P. Courtier, M. Ghil, A.C. Lorenc, Unified notation for data assimilation: Operational, sequential and variational, Journal of the Meteorological Society of Japan 75 (1B) (1997) 181–189.
[3] F. Bouttier, P. Courtier, Data assimilation concepts and methods, ECMWF, Meteorological Training Course Lecture Series, March 1999.
[4] F. Rabier, Overview of global data assimilation development in numerical weather-prediction centers, Quarterly Journal of the Royal Meteorological Society 131 (2005) 3215–3233.
[5] Special Issue on the Revolution in Global Ocean Forecasting. GODAE: 10 Years of Achievement, Oceanography Society, 2009, vol. 22.

[6] E. Kalnay, Atmospheric Modeling, Data Assimilation and Predictability, Cambridge University Press, 2003.
[7] J. Mandel, L.S. Bennethum, J.D. Beezley, J.L. Coen, C.D. Douglas, M. Kim, A. Vodacek, A wildland fire model with data assimilation, Mathematics and Computers in Simulation 79 (2008) 584–606.
[8] A. Gelb, Applied Optimal Estimation, MIT Press, Cambridge, MA, 1974.
[9] R. Todling, S.E. Cohn, Suboptimal schemes for atmospheric data assimilation based on the Kalman filter, Monthly Weather Review 122 (1994) 2530–2557.
[10] O. Talagrand, Assimilation of observations—An introduction, Journal of the Meteorological Society of Japan 75 (1B) (1997) 191–209.
[11] T. Poinsot, D. Veynante, Theoretical and Numerical Combustion, 2nd edition, R.T. Edwards, 2005.
[12] R.G. Rehm, R.J. McDermott, Fire front propagation using the level-set method, NIST, Technical Report 1611, 2009.
[13] M.J. Wooster, G. Roberts, G. Perry, Y.J. Kaufman, Retrieval of biomass combustion rates and totals from fire radiative power observations: FRP derivation and calibration relationships between biomass consumption and fire radiative energy release, Journal of Geophysical Research 110 (2005) D24311.
[14] R.C. Rothermel, A mathematical model for predicting fire spread in wildland fuels, USDA Forest Service, Research Paper INT-115, Intermountain Forest and Range Experiment, Ogden, UT:40, 1972.